Astronomy & Astrophysics manuscript no. fgvir6 February 2, 2008
(DOI: will be inserted by hand later)

arXiv:astro-ph/0502073v1 3 Feb 2005

Detection of 75+ pulsation frequencies in the δ Scuti star FG Vir

M. Breger[1], P. Lenz[1], V. Antoci[1], E. Guggenberger[1], R. R. Shobbrook[2], G. Handler[1], B. Ngwato[3], F. Rodler[1], E. Rodriguez[4], P. López de Coca[4], A. Rolland[4], and V. Costa[4]

[1] Institut für Astronomie der Universität Wien, Türkenschanzstr. 17, A–1180 Wien, Austria
e-mail: michel.breger@univie.ac.at
[2] Research School of Astronomy and Astrophysics, Australian National University, Canberra, ACT, Australia
[3] Theoretical Astrophysics Programme, University of the North-West, Private Bag X2046, Mmabatho 2735, South Africa
[4] Instituto de Astrofisica de Andalucia, CSIC, Apdo. 3004, E-18080 Granada, Spain

Received date; accepted date

Abstract. Extensive photometric multisite campaigns of the δ Scuti variable FG Vir are presented. For the years 2003 and 2004, 926 hours of photometry at the millimag precision level were obtained. The combinations with earlier campaigns lead to excellent frequency resolution and high signal/noise. A multifrequency analysis yields 79 frequencies. This represents a new record for this type of star. The modes discovered earlier were confirmed. Pulsation occurs over a wide frequency band from 5.7 to 44.3 c/d with amplitudes of 0.2 mmag or larger. Within this wide band the frequencies are not distributed at random, but tend to cluster in groups. A similar feature is seen in the power spectrum of the residuals after 79 frequencies are prewhitened. This indicates that many additional modes are excited. The interpretation is supported by a histogram of the photometric amplitudes, which shows an increase of modes with small amplitudes. The old question of the 'missing modes' may be answered now: the large number of detected frequencies as well as the large number of additional frequencies suggested by the power spectrum of the residuals confirms the theoretical prediction of a large number of excited modes.
FG Vir shows a number of frequency combinations of the dominant mode at 12.7162 c/d ($m = 0$) with other modes of relatively high photometric amplitudes. The amplitudes of the frequency sums are higher than those of the differences. A second mode (20.2878 c/d) also shows combinations. This mode of azimuthal order m = -1 is coupled with two other modes of m = +1.

Key words. stars: variables. δ Sct – Stars: oscillations – Stars: individual: FG Vir – Techniques: photometric

1. Introduction

The δ Scuti variables are stars of spectral type A and F in the main-sequence or immediate post-main-sequence stage of evolution. They generally pulsate with a large number of simultaneously excited radial and nonradial modes, which makes them well-suited for asteroseismological studies. The photometric amplitudes of the dominant modes in the typical δ Scuti star are a few millimag. It is now possible for ground-based telescopes to detect a large number of simultaneously excited modes with submillimag amplitudes in stars other than the Sun (e.g., Breger et al. 2002, Frandsen et al. 2001). Because photometric studies measure the integrated light across the stellar surface, they can detect low-degree modes only. This is a simplification for the interpretation because of fewer possibilities in mode identification.

A typical multisite photometric campaign allows the discovery of about five to ten frequencies of pulsation from about 200 to 300 hours of high-precision photometry (e. g., V351 Ori, Ripepi et al. 2003; V534 Tau, Li et al. 2004). These excellent observational studies are then compared to theoretical pulsation models, but the fit is hardly unique (e.g., θ^2 Tau, Breger et al. 2002b). The uniqueness problem can be lessened by studies with even lower noise in the power spectrum. This can be achieved by the very accurate measurements from space and by larger ground-based studies with more data, which concentrate on a single selected star. These more extensive ground-based studies also lead to to higher frequency resolution. The latter is important, because δ Scuti stars can show a large number of very close frequency pairs (or groups), which can only be resolved through long-term studies lasting many months or years. The question of frequency resolution is an important aspect in planning asteroseismological space missions (e.g., see Handler 2004, Garrido & Poretti 2004).

The Delta Scuti Network (DSN) is a network of telescopes situated on different continents. The collaboration reduces the effects of regular daytime observing gaps. The network is engaged in a long-term program (1000+ hours of observation, 10+ years, photometry and spectroscopy) to determine the structure and nature of the multiple frequencies of selected δ Scuti stars situated in different parts of the classical instability strip. The star FG Vir is the present main long-term target of the network. This 7500K star (Mantegazza, Poretti & Bossi 1994) is at the end of its main-sequence evolution. The projected rotational velocity is very small (21.3 ± 1.0 km s^{-1}, Mittermayer & Weiss 2003, see also Mantegazza & Poretti 2002).

A number of photometric studies of the variability of FG Vir are available: a lower-accuracy study by Dawson from the years 1985 and 1986 (Dawson, Breger & López de Coca 1995, data not used here), high-accuracy studies from 1992 (Mantegazza, Poretti & Bossi 1994), as well as previous campaigns by the Delta Scuti Network in 1993, 1995 and 2002 (Breger et al. 1995, 1998, 2004). Furthermore, for the year 1996, additional *uvby* photometry is available (Viskum et al. 1998). 12 nights of data were of high accuracy and could be included.

Because of the large scope of the long-term project on the pulsation of FG Vir, the photometric, spectroscopic and pulsation-model results cannot be presented in one paper. Here we present the extensive new photometric data from 2003 and 2004 as well as multifrequency analyses to extract the multiple frequencies excited in FG Vir. The analyses concentrate on the available three years of extensive coverage (2002–2004) and also consider the previous data (1992–1996).

Separate studies, presently in progress, will (i) present mode identifications based mainly on high-dispersion line-profile analyses and the data presented in this paper, (ii) examine the nature of close frequencies, (iii) compute asteroseismological models of stellar structure to fit the observed frequency spectrum.

2. New photometric measurements

During 2003 and 2004, photometric measurements of the star FG Vir were scheduled for $\sim$ 350 nights at four observatories. Of these, 218 nights were of high photometric quality at the millimag level with no instrumental problems. These are listed in Table 1 together with the additional details:

1. The APT measurements were obtained with the T6 0.75 m Vienna Automatic Photoelectric Telescope (APT), situated at Washington Camp in Arizona (Strassmeier et al. 1997, Breger & Hiesberger 1999). The telescope has been used before for several lengthy campaigns of the Delta Scuti Network, which confirmed the long-term stability and millimag precision of the APT photometry.
2. The OSN measurements were obtained with the 0.90 m telescope located at 2900m above sea level in the South-East of Spain at the Observatorio de Sierra Nevada in Granada, Spain. The telescope is equipped with a simultaneous four-channel photometer (*uvby* Strömgren photoelectric photometer). The observers for 2003 were: E. Rodriguez, P. López de Coca, A. Rolland, and V. Costa.
3. The SAAO measurements were made with the Modular Photometer attached to the 0.5 m and the UCT photometer attached to the 0.75 m telescopes of the South African Astronomical Observatory. The observers were V. Antoci, E. Guggenberger, G. Handler and B. Ngwato.
4. The 0.6-m reflector at Siding Spring Observatory, Australia, was used with a PMT detector. The observers were P. Lenz and R. R. Shobbrook.

The measurements were made with Strömgren v and y filters. Since telescopes and photometers at different observatories have different zero-points, the measurements need to be adjusted. This was done by zeroing the average magnitude of FG Vir from each site and later readjusting the zero-points by using the final multifrequency solution. The shifts were in the submillimag range. We also checked for potential differences in the effective wavelength at different observatories by computing and comparing the amplitudes of the dominant mode. No problems were found.

The measurements of FG Vir were alternated with those of two comparison stars. Details on the three-star technique can be found in Breger (1993). We used the same comparison stars as during the previous DSN campaigns of FG Vir, viz., C1 = HD 106952 (F8V) and C2 = HD 105912 (F5V). No variability of these comparison stars was found. The two comparison stars also make it possible to check the precision of the different observing sites. The residuals from the assumed constancy were quite similar, i.e., for the (C1–C2) difference we find a standard deviation of ± 3 mmag for all observatories and passbands except for ± 2 mmag (2004 SAAO75 v as well as y passbands) and ± 4 mmag (2004 APT75 v and 2003 OSN90 y measurements. The power spectrum of the C1–C2 differences does not reveal any statistically significant peaks.

The resulting light curves of FG Vir are shown in Figs. 1 and 2, where the observations are also compared with the fit to be derived in the next section.

3. Multiple frequency analysis

The pulsation frequency analyses were performed with a package of computer programs with single-frequency and multiple-frequency techniques (PERIOD04, Lenz & Breger 2005; http://www.astro.univie.ac.at/~dsn/dsn/Period04/), which utilize Fourier as well as multiple-least-squares algorithms. The latter technique fits up to several hundreds of simultaneous sinusoidal variations in the magnitude domain and does not rely on sequential prewhitening. The amplitudes and phases of all modes/frequencies are determined by minimizing the residuals between the measurements and the fit. The frequencies can also be improved at the same time.

Table 1. Journal of the PMT observations of FG Vir for 2003 and 2004

Start HJD	Length hours	Obs./ Tel.	Start HJD	Length hours	Obs./ Tel.	Start HJD	Length hours	Obs./ Tel.	Start HJD	Length hours	Obs./ Tel.
245 000+		Year 2003	2748.29	4.6	SAAO50	2788.89	4.5	SSO60	3108.63	4.8	APT75
2656.99	1.7	APT75	2748.64	6.5	APT75	2792.66	2.9	APT75	3109.62	6.9	APT75
2667.81	5.7	APT75	2748.89	4.9	SSO60	2796.66	2.7	APT75	3110.26	2.0	SAAO50
2668.91	3.6	APT75	2749.25	5.9	SAAO50	2798.67	2.3	APT75	3110.63	6.9	APT75
2670.81	5.8	APT75	2749.64	6.5	APT75	2802.66	2.4	APT75	3111.63	6.8	APT75
2671.64	0.7	OSN90	2749.89	6.7	SSO60	2803.66	2.3	APT75	3113.23	6.5	SAAO50
2673.79	6.1	APT75	2750.26	5.5	SAAO50	2805.66	2.2	APT75	3114.64	5.3	APT75
2674.61	3.4	OSN90	2750.70	5.0	APT75	2806.66	2.0	APT75	3115.63	6.5	APT75
2675.62	3.1	OSN90	2750.93	5.8	SSO60	2809.88	2.8	SSO60	3117.63	5.9	APT75
2676.63	3.0	OSN90	2751.36	2.9	OSN90	2812.66	1.6	APT75	3118.63	6.3	APT75
2677.78	4.4	APT75	2751.37	2.3	SAAO50	2813.66	1.8	APT75	3119.63	6.1	APT75
2686.81	0.7	APT75	2751.91	2.8	SSO60	2813.87	1.8	SSO60	3120.63	6.0	APT75
2692.75	6.0	APT75	2752.90	3.4	SSO60	2814.65	0.8	APT75	3123.74	3.2	APT75
2693.82	4.2	APT75	2753.24	6.0	SAAO50	2816.66	1.4	APT75	3125.63	5.8	APT75
2699.96	1.9	APT75	2753.64	6.2	APT75		Year 2004		3130.64	5.1	APT75
2703.77	1.8	APT75	2754.25	5.7	SAAO50	3022.83	5.3	APT75	3131.65	4.8	APT75
2706.71	7.3	APT75	2754.64	6.0	APT75	3023.83	5.0	APT75	3132.66	4.6	APT75
2707.72	1.5	APT75	2754.90	4.4	SSO60	3031.81	1.3	APT75	3136.64	4.8	APT75
2709.71	7.4	APT75	2755.25	5.4	SAAO50	3032.81	5.8	APT75	3137.25	3.1	SAAO50
2710.71	7.3	APT75	2755.66	5.5	APT75	3033.93	2.8	APT75	3137.64	4.7	APT75
2711.71	6.1	APT75	2756.25	5.5	SAAO50	3034.85	4.9	APT75	3138.23	2.7	SAAO50
2712.67	1.2	OSN90	2757.65	5.6	APT75	3035.82	5.1	APT75	3138.64	4.4	APT75
2713.70	4.0	APT75	2758.64	3.9	APT75	3049.98	1.6	APT75	3139.24	3.1	SAAO50
2714.44	3.1	OSN90	2758.95	4.6	SSO60	3051.00	1.0	APT75	3139.64	4.4	APT75
2719.77	5.3	APT75	2759.65	5.6	APT75	3051.80	5.9	APT75	3140.22	3.2	SAAO50
2720.02	2.4	SSO60	2759.88	4.8	SSO60	3052.76	5.9	APT75	3141.64	1.9	APT75
2720.81	4.2	APT75	2760.37	3.6	OSN90	3053.90	0.8	APT75	3142.22	3.1	SAAO50
2720.98	6.1	SSO60	2760.64	5.6	APT75	3057.74	7.2	APT75	3144.23	3.9	SAAO75
2721.68	7.4	APT75	2760.93	5.4	SSO60	3060.76	6.6	APT75	3145.74	1.6	APT75
2722.67	7.4	APT75	2761.72	3.7	APT75	3061.73	7.4	APT75	3146.20	1.7	SAAO75
2722.98	5.7	SSO60	2761.88	4.6	SSO60	3062.90	0.9	APT75	3146.65	3.3	APT75
2723.75	4.3	APT75	2762.36	4.1	OSN90	3064.73	6.8	APT75	3147.21	4.4	SAAO75
2724.69	6.8	APT75	2762.64	5.5	APT75	3075.69	1.9	APT75	3147.64	3.8	APT75
2725.76	5.0	APT75	2762.88	5.6	SSO60	3079.71	6.8	APT75	3148.64	3.7	APT75
2726.75	5.3	APT75	2763.36	3.6	OSN90	3080.72	6.5	APT75	3149.65	3.7	APT75
2727.66	6.7	APT75	2764.65	4.8	APT75	3081.68	7.6	APT75	3152.20	4.1	SAAO75
2729.64	7.6	APT75	2765.65	4.0	APT75	3082.67	7.7	APT75	3153.65	3.3	APT75
2729.95	1.5	SSO60	2766.75	2.5	APT75	3086.74	4.8	APT75	3155.20	3.1	SAAO75
2730.64	7.6	APT75	2768.03	0.6	SSO60	3087.66	7.6	APT75	3156.19	4.0	SAAO75
2733.64	7.4	APT75	2768.65	4.9	APT75	3088.79	4.6	APT75	3157.30	1.5	SAAO75
2734.63	7.6	APT75	2769.36	3.6	OSN90	3090.84	0.8	APT75	3160.65	1.7	APT75
2735.63	7.5	APT75	2769.89	1.7	SSO60	3091.65	3.9	APT75	3161.65	2.7	APT75
2735.99	1.2	SSO60	2770.36	2.3	OSN90	3092.66	7.3	APT75	3162.65	2.7	APT75
2736.63	7.4	APT75	2771.08	1.2	SSO60	3093.64	7.5	APT75	3163.65	2.1	APT75
2736.94	1.0	SSO60	2775.65	4.1	APT75	3094.66	7.1	APT75	3165.65	2.4	APT75
2737.63	7.3	APT75	2776.65	4.5	APT75	3095.37	2.4	SAAO50	3166.65	2.3	APT75
2738.64	4.1	APT75	2777.75	1.9	APT75	3101.24	6.8	SAAO50	3167.65	2.5	APT75
2740.65	6.7	APT75	2778.65	4.0	APT75	3102.24	6.8	SAAO50	3168.65	2.5	APT75
2743.99	4.4	SSO60	2779.66	4.0	APT75	3102.73	4.9	APT75	3171.65	2.2	APT75
2744.28	5.1	SAAO50	2781.65	4.1	APT75	3103.63	7.3	APT75	3172.65	2.2	APT75
2745.26	1.8	SAAO50	2784.67	3.3	APT75	3104.62	0.7	APT75	3173.65	2.1	APT75
2745.90	4.6	SSO60	2785.65	3.8	APT75	3106.26	6.1	SAAO50	3174.65	1.8	APT75
2747.10	1.7	SSO60	2785.90	3.2	SSO60	3107.28	5.8	SAAO50	3175.65	1.9	APT75
2747.66	6.1	APT75	2786.67	2.5	APT75	3107.65	6.6	APT75	3177.65	1.8	APT75
2747.94	5.3	SSO60	2787.66	1.9	APT75	3108.24	6.7	SAAO50	3187.65	1.0	APT75

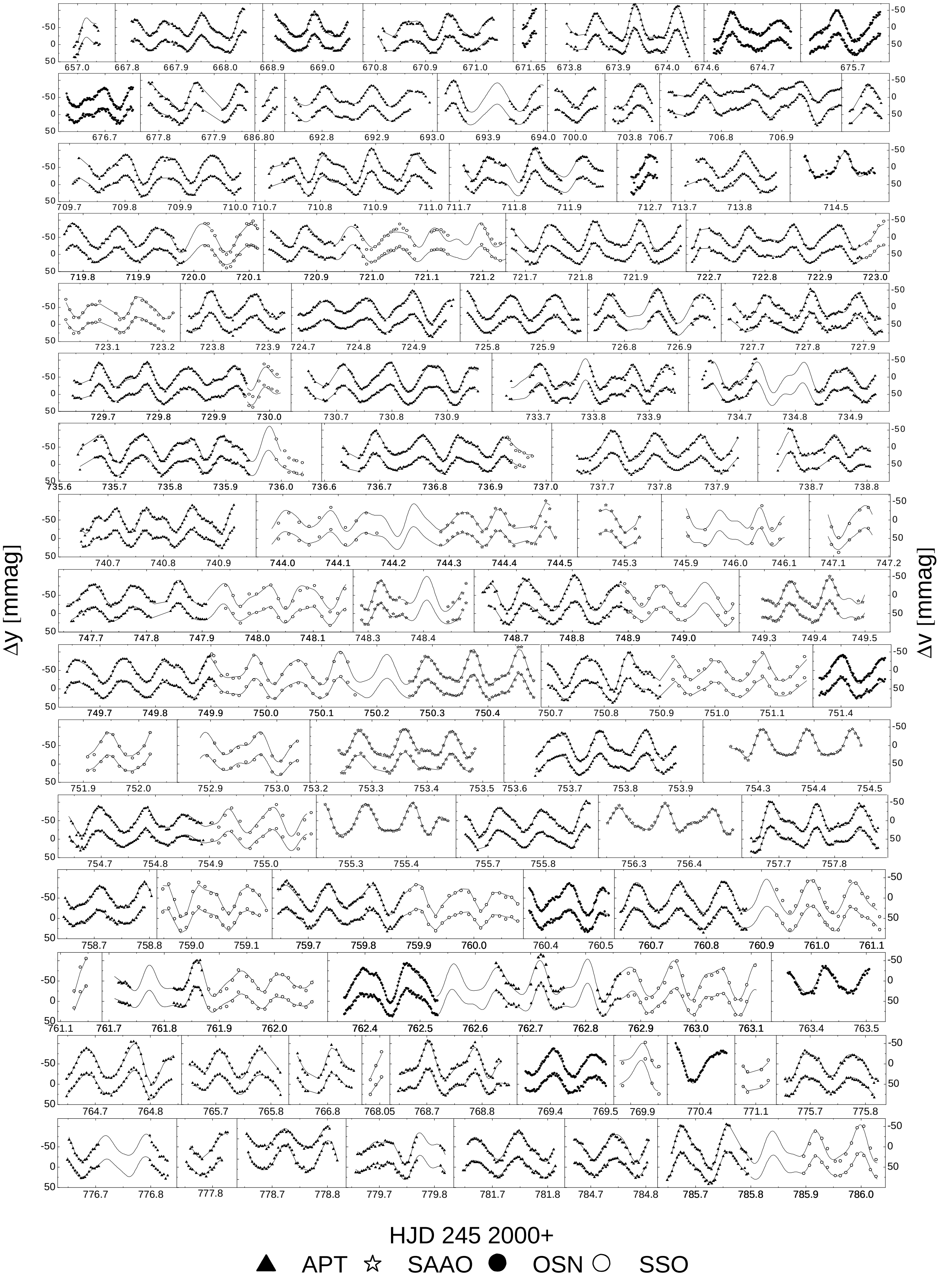

Fig. 1. Multisite photoelectric three-star-photometry of FG Vir obtained during the 2003 and 2004 DSN campaigns. Δy and Δv are the observed magnitude differences (variable – comparison stars) normalized to zero in the narrowband *uvby* system. The fit of the 79 frequency solution derived in this paper is shown as a solid curve. Note the excellent

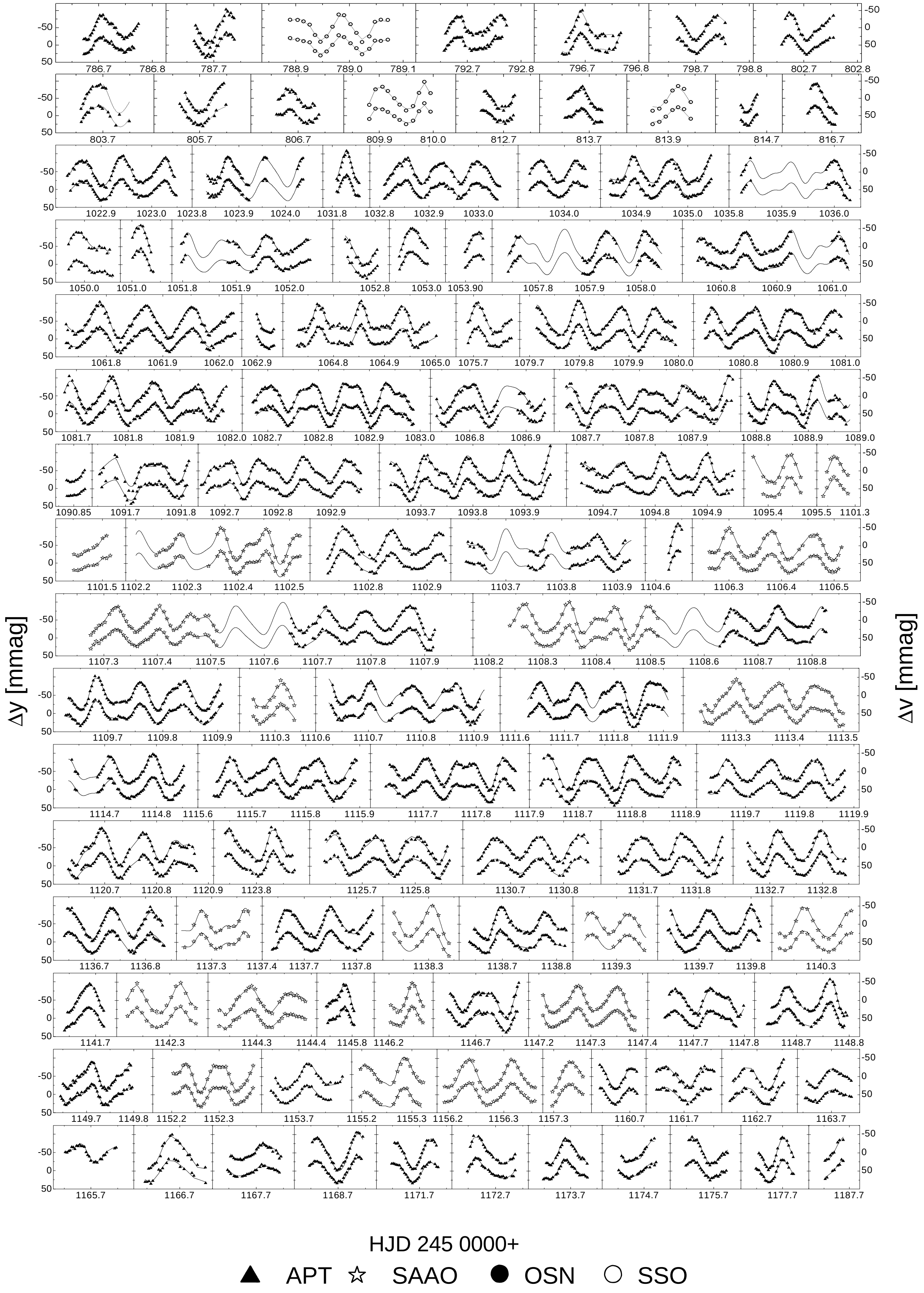

Fig. 2. Multisite photoelectric three-star-photometry of FG Vir obtained during the 2003 and 2004 DSN campaigns, continued

The file of the figure is too large to be uploaded to astro-ph.

Please download the complete paper from

http://www.astro.univie.ac.at/~dsn/dssn/news2005/fgvir.pdf

Fig. 3. Example of power spectra of the 1992–2004 data. Top: Spectral windows showing effects of the daily and annual aliasing. Bottom: New frequencies detected in the most difficult frequency region with the lowest amplitudes. The diagram shows that in the 40–45 c/d region pulsation modes are present and have been detected. The choice of which peaks are statistically significant depends somewhat on the details of the analysis.

Our analysis consists of two parts: We first examine the extensive 2002 - 2004 data and then add the available 1992 - 1996 data.

3.1. Frequencies detected in the 2002 - 2004 data

The following approach was used in an iterative way:

(i) The data were divided into two data sets to separate the y and v filters, each covering the total time period from 2002 - 2004. This is necessary because the amplitudes and phasing of the pulsation are strongly wavelength dependent. In principle, the different amplitudes could be compensated for by multiplying the v data by an experimentally determined factor of 0.70 and increasing the weights of the scaled v data accordingly. (Anticipating the results presented later in Table 2, we note that this ratio is confirmed by the average amplitude ratio of the eight modes with highest amplitudes.) However, the small phase shifts of a few degrees cannot be neglected for the larger-amplitude modes. Consequently, the data were analyzed together for exploratory analysis, but not for the final analyses.

(ii) We started with the single-frequency solution for the two data sets using the program PERIOD04. For the Fourier analyses the two data sets were combined to decrease the noise, while for the actual fits to the data, separate solutions were made.

(iii) A Fourier analysis was performed to look for additional frequencies/modes from the combined residuals of the previous solutions. Additional frequencies were then identified and their signal/noise ratio calculated. Following Breger et al. (1993), a significance criterion of amplitude signal/noise = 4.0 (which corresponds to power signal/noise of ∼12.6) was adopted for non-combination frequencies. The most clearly detected additional frequencies were included in a new multifrequency solution. In order for a new frequency to be accepted as real, the signal/noise criterion also had to be fulfilled in the multifrequency solution. This avoids false detections due to spill-over effects because the Fourier technique is a single-frequency technique. Furthermore, since there exist regular annual gaps, trial annual alias values (separated by 0.0027 c/d) were also examined. We note that the choice of an incorrect annual alias value usually has little or no effect on the subsequent search for other frequencies. The choice of an incorrect daily alias (separated by 1 c/d) would be more serious and we carefully examined different frequency values.

(iv) The previous step was repeated adding further frequencies until no significant frequencies were found. Note that only the Fourier analyses assume prewhitening; the multiple-frequency solutions do not.

In this paper we omit the presentation of very lengthy diagrams showing the sequential detection of new frequencies, except for the example shown in the next subsection. A detailed presentation of our approach and its results can be found in our analysis of the 2002 data (Breger et al. 2004).

FG Vir contains one dominant frequency: 12.7162 c/d with a photometric amplitude five times higher than that of the next strongest mode. To avoid potential problems caused by even small amplitude variability, for this frequency we calculated amplitudes on an annual basis. The results of the multifrequency analysis are shown in Table 2. The numbering scheme of the frequencies corresponds to the order of detection, i.e., the amplitude signal/noise ratio, and therefore differs from that used in previous papers on FG Vir.

3.2. Further frequencies detected in the 1992 - 2004 data

An extensive photometric data set covering 13 years is essentially unique in the study of δ Scuti stars, promising new limits in frequency resolution and noise reduction in Fourier space. The noise reduction is especially visible at high frequencies, where the effects of systematic observational errors are small. The analysis of the combined data had to work around two problems: the earlier data is not as extensive as the 2002 - 2004 data and there exists a large time gap between 1996 and 2002.

The time gap did lead to occasional uniqueness problems for the frequencies with amplitudes in the 0.2 mmag range: next to the annual aliasing of 0.0027 c/d we find peaks spaced 0.00026 c/d, corresponding to a ∼ 10 year spacing (see Fig. 3, top right). Fortunately, the excellent coverage from 2002 - 2004 minimized these ambiguities.

The relatively short coverage of the data from 1992 and 1996 excluded the computation of 79-frequency solutions for individual years (to avoid overinterpretation). We have consequently combined all the y measurements from 1992 to 1996 as well as the available 1995 and 1996 v data. Together with the y and v data sets from 2002 - 2004, we had four data sets.

Fig. 3 illustrates some examples of the resulting power spectra. Due to the large amount of APT data from 2002 - 2004, which therefore dominates, the 1 c/d aliases are not zero (top left). Nevertheless, due to the excellent frequency resolution, these aliases are very narrow so that the aliasing problem is not severe. The figure also shows the power spectrum of the measurements in the 40 - 45 c/d region, which was the most difficult region for us to analyze due to the small amplitudes of all the detected frequencies.

The new detections are included in Table 2.

A comparison with the frequencies published in earlier papers shows that all the previously detected frequencies were confirmed. This also includes those previously detected modes not found to be statistically significant in the 2002 data alone. In a few cases, different *annual* aliases were selected. However, the main result is the increase in the number of detected frequencies to 79, which more than doubles the previous results.

Fig. 4 shows the distribution of frequencies in frequency space. We note the wide range of excited frequencies, which is unusual for δ Scuti stars, as well as the clustering of the excited frequencies. This clustering persists even after the suspected combination frequencies and 2f harmonics are removed.

A new feature is the detection of frequencies with values between 40 and 45 c/d. They all have small amplitudes of $\Delta y \sim 0.2$ mmag. The lower noise of the new data now made their detection possible.

3.3. Color effects

The light curves of pulsating stars are not identical at different wavelengths. In fact, amplitude ratios and phase shifts provide a tool for the identification of nonradial modes (e.g., see Garrido et al. 1990, Moya et al. 2004). For δ Scuti stars, the amplitude ratios between different colors are primarily dependent on the surface temperature. For the individual pulsation modes, the phase differences and deviations from the *average* amplitude ratio are small. This means that observational errors need to be small and any systematic errors between the different colors should be avoided.

For most nights there exist both v and y passband data, so that amplitude ratios as well as phase differences can be derived. However, our 79-frequency solution is not perfect. In order not to introduce systematic errors in the phase differences and amplitude ratios, for the calculation of amplitude ratios and phase differences, we have omitted those nights for which two-color data are not available. Consequently, no data from 1992 and 1993 were used and all 1995 (single-color) CCD measurements were omitted.

Table 3 lists the derived phase differences and amplitude ratios for the modes with relatively high amplitudes. The uncertainties listed were derived from error-propagation calculations based on the standard formulae given by Breger et al. (1999). The results can now be used together with spectroscopic line-profile analyses to identify the pulsation modes.

4. Combination frequencies

We have written a simple program to test which of the 79 frequencies found can be expressed as the sum or differences of other frequencies. Due to the excellent frequency resolution of the 2002 - 2004 data, we could be very restrictive in the identification of these combinations. A generous limit of ± 0.001 c/d was adopted. The probability of incorrect identifications is correspondingly small. A number of combinations was found and these are marked in Table 2. They generally agreed to ± 0.0002 c/d.

How many accidental agreements do we expect? We have calculated this number through a large number of numerical simulations, assuming a reasonable agreement

Table 2. Frequencies of FG Vir from 2002 to 2004

Frequency			Detection(1)	Amplitude		Frequency			Detection	Amplitude	
cd^{-1}	Name	Type	Amplitude S/N ratio	v filter millimag	y filter	cd^{-1}	Name	Type	Amplitude S/N ratio	v filter millimag	y filter
				± 0.04	±0.05					± 0.04	±0.05
5.7491	f_{47}		5.7	0.48	0.28	23.3974	f_{12}	(2)	22	1.73	1.25
7.9942	f_{44}		5.9	0.42	0.34	23.4034	f_4	(2)	71	5.65	4.02
8.3353	f_{78}	f_6-f_1	*3.8*	0.33	0.17	23.4258	f_{53}		4.9	0.37	0.28
9.1991	f_7		53	3.82	2.78	23.4389	f_{24}		9.0	0.68	0.52
9.6563	f_5		71	5.20	3.61	23.8074	f_{48}		5.5	0.45	0.32
10.1687	f_{25}		8.6	0.64	0.42	24.0040	f_{58}		4.6	0.35	0.31
10.6872	f_{79}	f_4-f_1	3.5	0.26	0.15	24.1940	f_{10}		29	2.26	1.58
11.1034	f_{20}		11	0.67	0.65	24.2280	f_3		74	5.79	4.20
11.2098	f_{38}		6.4	0.35	0.43	24.3485	f_{18}		12	0.99	0.63
11.5117	f_{70}	f_3-f_1	4.0	0.30	0.18	24.8703	f_{36}	f_1+f_2	6.4	0.48	0.38
11.6114	f_{50}		5.3	0.35	0.27	25.1788	f_{30}		7.3	0.59	0.39
11.7016	f_{33}		6.9	0.42	0.44	25.3793	f_{45}		5.7	0.37	0.31
11.8755	f_{63}		4.4	0.27	0.25	25.4324	f_{15}	$2f_1$	16	1.23	0.89
11.9421	f_{29}		7.6	0.55	0.38	25.6387	f_{68}		4.0	0.30	0.26
12.1541	f_2	(2)	85	6.09	4.21	26.5266	f_{71}		*4.7*	0.30	0.20
12.1619	f_{14}	(2)	16	1.13	0.83	26.8929	f_{61}		4.5	0.34	0.27
12.2158	f_{52}		5.1	0.38	0.24	26.9094	f_{75}		*4.2*	0.34	0.19
12.7162	f_1		442	31.74	21.92	28.1359	f_{19}		11	0.87	0.55
12.7944	f_{17}		13	0.88	0.66	29.4869	f_{51}	f_7+f_{11}	5.2	0.39	0.28
13.2365	f_{27}		8.3	0.45	0.56	30.9146	f_{60}		4.5	0.31	0.27
14.7354	f_{49}		5.3	0.29	0.38	31.1955	f_{57}		4.6	0.35	0.27
16.0711	f_{13}		20	1.56	1.07	31.9307	f_{34}		6.6	0.49	0.40
16.0909	f_{31}		7.3	0.55	0.39	32.1895	f_{32}		7.0	0.56	0.38
19.1642	f_{26}		8.6	0.55	0.59	33.0437	f_{74}	(4)	*4.3*	0.29	0.19
19.2278	f_9		30	2.51	1.69	33.7677	f_{43}	f_1+f_6	5.9	0.44	0.31
19.3259	f_{41}		6.3	0.53	0.34	34.1151	f_{22}		9.8	0.75	0.49
19.6439	f_{65}		4.3	0.40	0.22	34.1192	f_{72}		*4.7*	0.21	0.25
19.8679	f_8	(3)	55	4.44	3.19	34.1864	f_{54}		4.9	0.37	0.25
19.8680		(3)	30	2.40	1.78	34.3946	f_{55}		4.6	0.31	0.28
20.2878	f_{11}		26	2.13	1.45	34.5737	f_{23}		9.3	0.69	0.45
20.2925	f_{56}		4.6	0.31	0.39	35.8858	f_{76}		*4.1*	0.22	0.21
20.5112	f_{35}		6.6	0.41	0.52	36.1196	f_{40}	f_1+f_4	6.3	0.40	0.31
20.8348	f_{39}		6.3	0.53	0.38	36.9442	f_{37}	f_1+f_3	6.4	0.43	0.27
21.0515	f_6		55	4.43	3.08	39.2165	f_{69}		4.0	0.27	0.16
21.2323	f_{16}		14	1.06	0.80	39.5156	f_{59}	f_9+f_{11}	4.5	0.24	0.25
21.4004	f_{46}		5.7	0.52	0.33	42.1030	f_{64}	$2f_6$	4.3	0.22	0.28
21.5507	f_{28}		7.9	0.61	0.42	42.1094	f_{62}		4.5	0.24	0.25
22.3725	f_{42}	f_1+f_5	6.2	0.52	0.35	43.0134	f_{73}		*4.4*	0.21	0.15
23.0253	f_{66}		4.1	0.30	0.23	43.9651	f_{67}		4.0	0.26	0.17
23.3943	f_{21}		11	0.85	0.60	44.2591	f_{77}		*4.0*	0.20	0.18

(1) The noise for the amplitude signal/noise ratios were calculated over a 4 cd^{-1} range. Limits for a significant detection are 4.0 for independent frequencies and 3.5 for combination modes with known values. Numbers in italics indicate 1992 - 2004 data (see text).

(2) The close frequencies, 12.1541 and 12.1619 as well as 23.3974 and 23.4034 c/d, are all separate modes. In short data sets this could lead to an erroneous identification as single modes with variable amplitude.

(3) For the possible frequency pair near 19.868 c/d the existence of two separate modes cannot be proved at this point. A single frequency with a slowly variable amplitude (beat period ~21.5 years) is also possible.

(4) The 2002–2004 data clearly show a mode at 33.044 c/d, though with considerably reduced amplitudes from 1992-1995 data. Breger et al. (1998) listed the value of the frequency as 33.056 c/d, which was the highest peak from a broad selection of peaks separated by annual aliases 0.0027 c/d apart. We note that in the new data, a value separated by 1 annual alias, viz., 33.0461 c/d, is also possible.

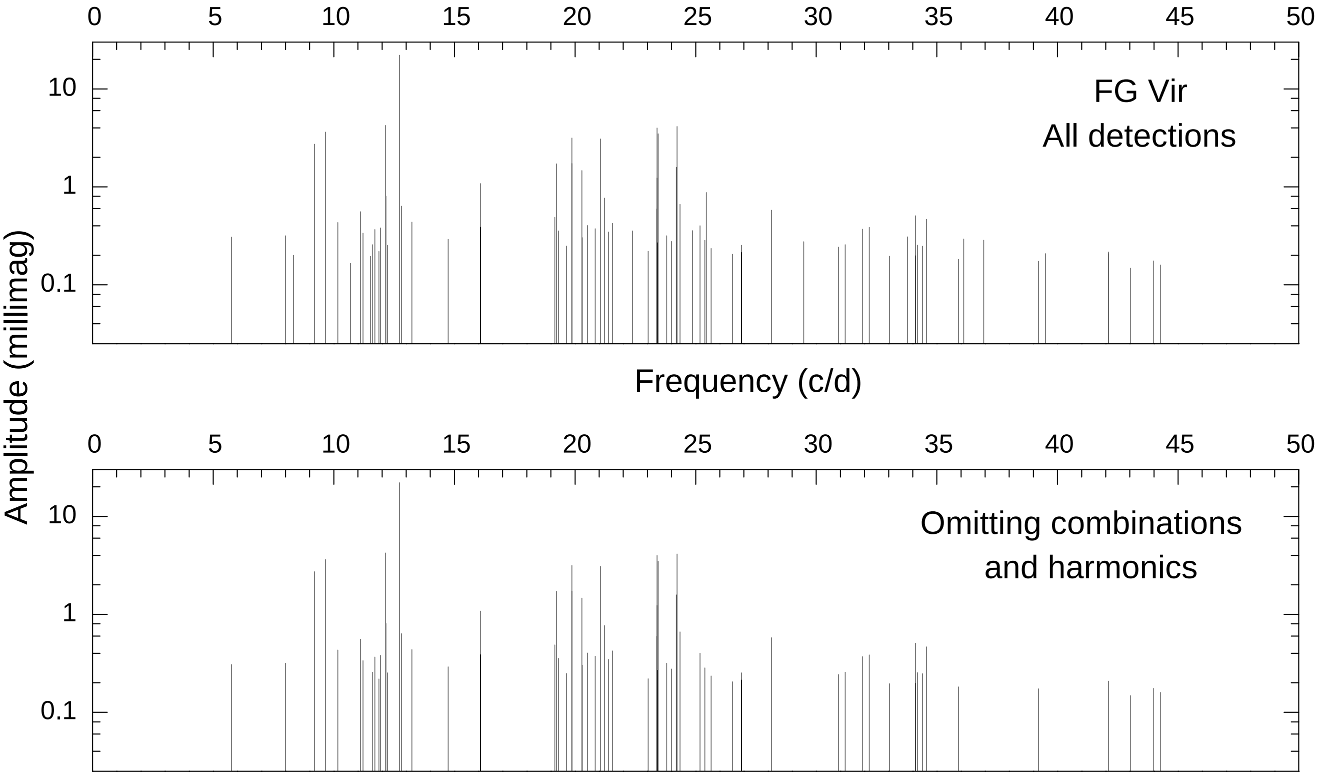

Fig. 4. Distribution of the frequencies of the detected modes. The diagram suggests that the excited pulsation modes are not equally distributed in frequency.

Table 3. Phase differences and amplitude ratios

Frequency c/d		Phase differences in degrees $\phi_v - \phi_y$ 2002–2004	1995–2004[1)]	Amplitude ratios v/y 2002–2004	1995–2004
f_1	12.716	–1.7 ± 0.1	–1.5	1.45 ± 0.00	1.45
f_2	12.154	+3.1 ± 0.7	+2.8	1.44 ± 0.02	1.44
f_3	24.227	–3.0 ± 0.7	–3.0	1.38 ± 0.02	1.40
f_4	23.403	–3.5 ± 0.7	–3.3	1.40 ± 0.02	1.42
f_5	9.656	–5.1 ± 0.8	–4.5	1.44 ± 0.02	1.43
f_6	21.051	–3.7 ± 1.0	-4.2	1.44 ± 0.02	1.45
f_7	9.199	–6.7 ± 1.1	–6.6	1.38 ± 0.03	1.40
f_8	19.868[2)]	–4.3 ± 1.9	–2.9	1.45 ± 0.05	1.44
f_9	19.228	–4.6 ± 1.7	–3.9	1.48 ± 0.05	1.46
f_{10}	24.194	–1.2 ± 1.9	-0.6	1.43 ± 0.07	1.38

[1)] Error estimates omitted: usually lower than for 2002–2004, but some instability is possible due to large time gap
[2)] Using single frequency with annual amplitude variations

of the observed frequency to within 0.0002 c/d of the predicted frequency. We obtain an average of 0.93 accidental matchings of peaks with combination frequencies. We conclude that most or all detected combination frequencies are not accidental. The argument is strengthened by the fact that the combinations detected by us all contain one of two specific modes, which reduces the chance of accidental agreements to essentially zero.

We also note that the lowest frequency detected, f_{47} at 5.749 c/d, can be expressed as a *triple* combination of f_1, f_3 and f_{57}. This may be accidental.

4.1. Combinations of the dominant mode at 12.7163 c/d

Due to the presence of a dominant mode at 12.7163 c/d (f_1), it is not surprising that some combination frequencies, $f_1 \pm f_i$, exist and are detected (see Table 2). In order

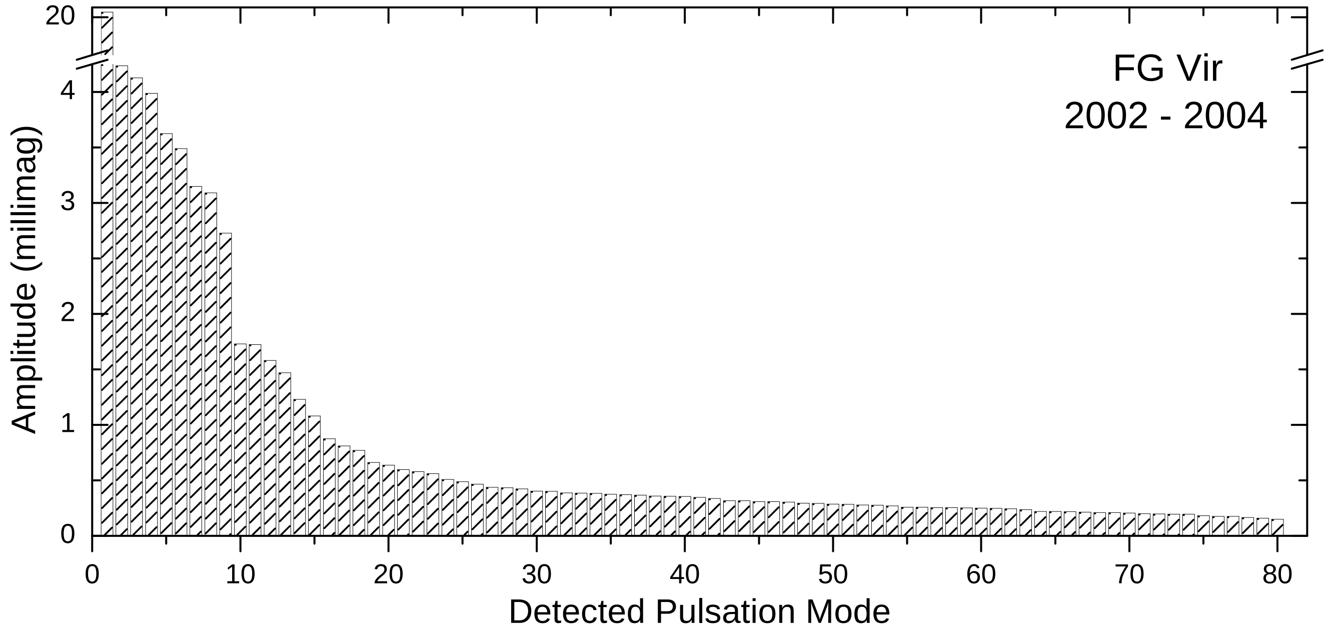

Fig. 5. Distribution of the amplitudes of the frequencies with significant detections. To increase the accuracy, we have computed amplitudes from 0.5*(y amplitude + 0.70 v amplitude) to simulate the amplitude in the y passband. Note the large number of detected modes with amplitudes near the detection limit of 0.2 mmag. This suggests that even moderate increases in the amount of data lead to considerably higher number of detections.

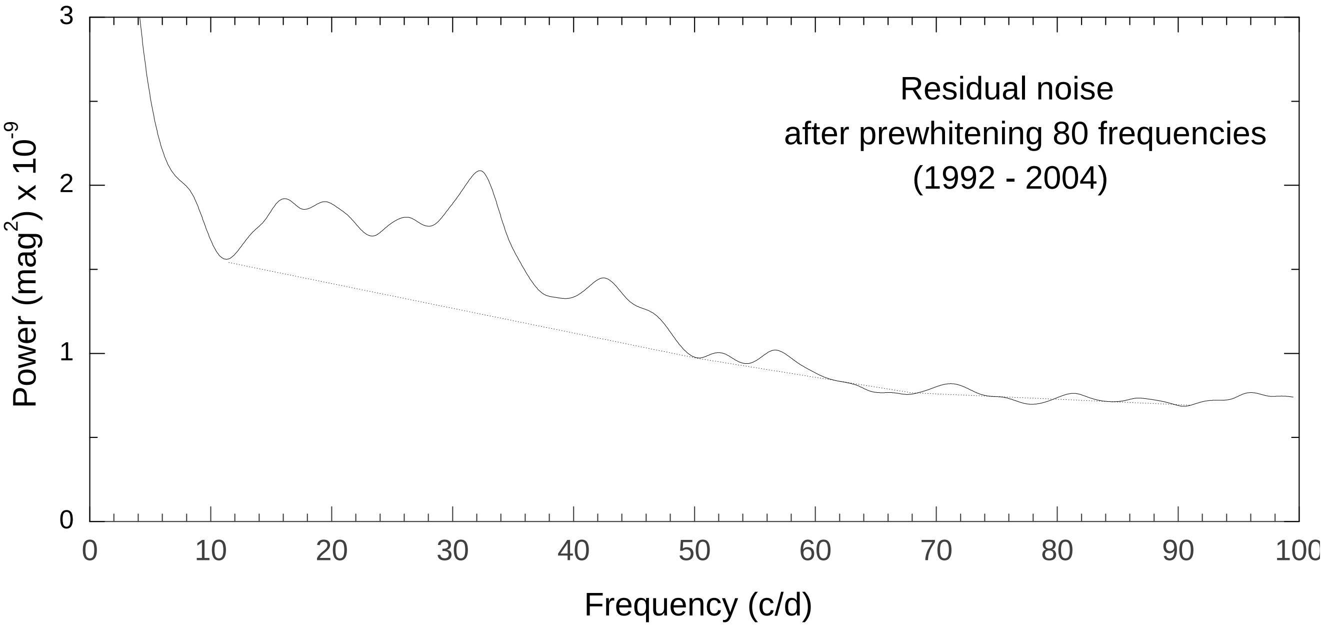

Fig. 6. Power of the residual noise of the 1992 – 2004 data after subtracting 80 (79) frequencies. (The additional frequency is the close doublet at 19.868 c/d adopted for the long time span.) The average amplitude in the amplitude spectrum was calculated for 2 c/d regions and squared to give power. The strong increase towards lower frequencies is caused by observational noise and standard in terrestrial photometry. Note the excess power in 10 - 50 c/d region, shown above the dotted curve. This shows that many additional pulsation modes exist in the same frequency region in which the already detected frequencies occur.

to examine this further, we have performed additional calculations with the 2002 - 2004 data. We have repeated our multifrequency solutions described earlier while omitting all frequency combinations of f_1. The residuals of the y and v data were combined to form the sum (y + 0.70v) to account for the different amplitudes at the two passbands. A new multifrequency solution containing the possible combinations of the dominant mode with f_2 through f_8 was made. The results are shown in Table 4, in which small differences compared to Table 2 are caused by the different

Table 4. Combination frequencies involving the dominant mode

$f_1\pm$	Amplitude in y (2002–2004) Sum of frequencies mmag	 Difference of frequencies mmag
f_2	0.35	(0.06)
f_3	0.28	0.19
f_4	0.31	0.17
f_5	0.33	(0.16)
f_6	0.39	0.21
f_7	(0.10)	(0.07)
f_8	(0.07)	(0.13)

The amplitudes in brackets are too low for fulfilling the adopted criterion of statistical significance.

procedures of our analyses. The amplitudes of the sums (f_1+f_i) are higher than those of the differences (f_1-f_i). We believe the result to be real and intrinsic to the star. The differences are generally found at low frequencies, where the observational noise is higher. Increased noise should lead to higher amplitudes, which are not found.

4.2. Combinations of the 20.2878 c/d mode

Apart from the mode combinations involving the dominant mode, f_1, two other two-mode combinations are found, both involving f_{11} at 20.2878 c/d. While the mode identifications are still in progress, this mode can to a high probability be identified as a ℓ=1, m=-1 mode (Zima et al. 2003). At first sight, this appears surprising, since the photometric amplitude is only 1.5 mmag. However, for the known inclination and mode identification, we calculate a geometric cancellation factor of ~3.6, so that the real amplitude of this mode is 5 mmag or larger.

The fact that the m value is not equal to zero has some interesting consequences for the observations of combination frequencies. The reason is that there are two frames of reference: the stellar frame corotating with the star, and that of the observer. For nonradial modes of m values $\neq 0$ (i.e., waves traveling around the star), the frequencies between the two frames of reference differ by $m\Omega$, where Ω is the rotation frequency of the star (see Cox 1984 for an excellent discussion). The frequency combinations occur in the corotating (stellar) frame, and not the observer's frame of reference. Consequently, many possible combinations involving non-axisymmetric modes should not be observed as simple sums or differences of observed frequency values.

It follows that for the non-axisymmetric (m=-1) mode at 20.2878 c/d, our simple method to search for combination frequencies from the observed frequency values may only detect combinations, $f_i + f_j$, with $m = +1$ modes.

This strict requirement is met by the two identified combinations of 20.2878 c/d! Both coupled modes, $f_9 = 19.2278$ c/d as well as $f_{11} = 20.2878$ c/d have been identified as $m = +1$ modes. Such a combination of m values of opposite sign can be detected because the combination is invariant to the transformation between the two frames of reference: $-m\Omega + m\Omega = 0$.

5. The problem of missing frequencies solved?

δ Scuti star models predict pulsational instability in many radial and nonradial modes. The observed number of low-degree modes is much lower than the predicted number. The problem of mode selection is most severe for post-main-sequence δ Scuti stars, which comprise about 40 percent of the observed δ Scuti stars. The theoretical frequency spectrum of unstable modes is very dense. Most modes are of mixed character: they behave like p-modes in the envelope and like g-modes in the interior. For example, for a model of the relatively evolved star 4 CVn, the models predict 554 unstable modes of $\ell = 0$ to 2, i.e., 6 for $\ell = 0$, 168 for $\ell = 1$, and 380 for $\ell = 2$ (see Breger & Pamyatnykh 2002). However, only 18 (and additional 16 combination frequencies) were observed (Breger et al. 1999). The problem also exists for other δ Scuti stars. A complication occurs since the models so far cannot predict the amplitudes of the excited modes.

Two explanations offer themselves: the missing modes exist, but have amplitudes too small to have been observed, or there exists a mode selection mechanism, which needs to be examined in more detail. Promising scenarios involve the selective excitation of modes trapped in the envelope (Dziembowski & Królikowska 1990) or random mode selection.

Let us turn to the star FG Vir. Unpublished models computed by A. A. Pamyatnykh predict 80 unstable modes with $\ell = 0$, 1 and 2 in the 8 - 40 c/d range. This number is smaller than that mentioned previously for the more evolved star 4 CVn, but until now this large number was not observed either. The present study addresses the question by lowering the observational amplitude threshold to 0.2 mmag. We have detected 79 frequencies, of which 12 could be identified as harmonics or combination frequencies. This leaves 67 independent frequencies. There also exists considerable evidence that many more modes are excited:

(i) Consider the amplitude distribution of the detected modes shown in Fig. 5. There is a rapid increase in the number of modes as one goes towards low amplitudes. The present limit near 0.2 mmag is purely observational. Consequently, the number of excited modes must be much larger.

(ii) Consider the power spectrum of the residuals after subtraction of the multifrequency solution (Fig. 6). We see excess power in the 10 - 50 c/d range. This is exactly the region in which the previously detected modes were found. This indicates that many additional modes similar to the ones detected previously are excited at small amplitude.

We can exclude the possibility that the large number of observed frequencies is erroneous because of imperfect prewhitening due to amplitude variability. We have examined this possibility in great detail, with literally thousands of different multifrequency solutions allowing for amplitude variability. In no case was it possible to significantly reduce the structure in the power spectrum of the residuals. In fact, the 'best' multifrequency solution adopted treated the two colors as well as the 1992 - 1996 and 2002 - 2004 data separately and allowed annual amplitude variability of the dominant mode at 12.7162 c/d. Amplitude variability, therefore, cannot explain the excess power.

Consequently, the problem that the number of detected modes is much smaller than the number of predicted low-ℓ modes no longer exists, at least for FG Vir. Of course, we cannot conclude that each theoretically predicted mode is really excited and has been detected. This would require much more extensive mode identifications than are available at this stage.

In the previous discussion, we have concentrated on the low-ℓ modes which are easily observed photometrically. One also has to consider that at low amplitudes, variability from modes of higher ℓ values might also be seen photometrically. The geometric cancellation effects caused by the integration over the whole surface only become important for $\ell \geq 3$. This is shown by Daszyńska-Daszkiewicz et al. (2002), who calculated the amplitude reduction factors caused by temperature variations across the disk. From this paper we can roughly estimate a cancellation factor of ~50 in the y passband for $\ell = 3$ modes, implying that only the largest-amplitude modes could be photometrically detected. Such modes would have amplitudes similar to, or larger, than that of the observed dominant ($\ell = 1$) mode at 12.7162 c/d and might therefore be expected to be few. Regrettably, the situation is somewhat more complicated. The results presented in Fig. 2 of the Daszyńska-Daszkiewicz et al. paper are actually based on models with higher surface temperatures and could fit the β Cep variables. A. Pamyatnykh has kindly calculated specific models fitting the star FG Vir. Here the geometric cancellation factor becomes smaller by a factor of two or three. Consequently, some of the low-amplitude modes observed by us could also be $\ell = 3$ modes.

We conclude that the large number of detected frequencies as well as the large number of additional frequencies suggested by the power spectrum of the residuals confirms the theoretical prediction of a large number of excited modes. A mode-by-mode check for each predicted mode is not possible at this stage.

Acknowledgements

This investigation has been supported by the Austrian Fonds zur Förderung der wissenschaftlichen Forschung. The Spanish observations were supported by the Junta de Andaluca and the DGI under project AYA2000-1580. We are grateful to P. Reegen for help with the APT measurements, M. Viskum for providing a table of the individual measurements of the 1996 photometry not listed in his paper, A. A. Pamyatnykh and J. Daszyńska-Daszkiewicz for preliminary pulsation models, as well as W. Dziembowski and W. Zima for important discussions.

References

Breger, M., 1993, in Stellar Photometry - Current Techniques and Future Developments, ed. C. J. Butler, I. Elliott, IAU Coll. 136, 106

Breger, M., & Pamyatnykh, A. A. 2002, ASP Conf Ser., 259, 388

Breger, M., & Hiesberger, F. 1999, A&AS, 135, 547

Breger, M., Stich, J., Garrido, R., et al. 1993, A&A, 271, 482

Breger, M., Handler, G., Nather, R. E., et al. 1995, A&A, 297, 473

Breger, M., Zima, W., Handler, G., et al. 1998, A&A, 331, 271

Breger, M., Handler, G., Garrido, R., et al. 1999, A&A, 349, 225

Breger, M., Garrido, R., Handler, G., et al. 2002a, MNRAS, 329, 531

Breger, M., Pamyatnykh, A. A., Zima, W., et al. 2002b, MNRAS, 336, 249

Breger, M., Rodler, F., Pretorius, M. L., et al. 2004, A&A, 419, 695

Cox, J. P. 1984, PASP, 96, 577

Daszyńska-Daszkiewicz, J., Dziembowski, W. A., Pamyatnykh, A. A., & Goupil, M.-J., et al. 2002, A&A, 392, 151

Dawson, D. W., Breger., M., & López de Coca, P. 1995, PASP, 107, 517

Dziembowski, W., Królikowska, M., 1990, Acta Astron, 40, 19

Frandsen,S., Pigulski,A., Nuspl,J., et al. 2001, A&A,376, 175

Garrido, R., & Poretti, E. 2004, ASP Conf. Ser., 310, 560

Garrido, R., Garcia-Lobo, E., & Rodriguez, E. 1990, A&A, 234, 262

Handler, G. 2004, ESA SP-538, 127

Lenz, P., & Breger, M. 2005, CoAst, in press

Li, Z.-P., Michel, E., Fox Machado, L., et al. 2004, A&A, 420, 283

Mantegazza, L., & Poretti, E. 2002, A&A, 396, 911

Mantegazza, L., Poretti, E., & Bossi, M. 1994, A&A, 287, 95

Mittermayer, P., & Weiss, W. W. 2003, A&A, 407, 1097

Moya, A., Garrido, R., & Dupret, M. A. 2004, A&A, 414, 1081

Ripepi, V., Marconi, M., Bernabei, S., et al. 2003, A&A, 1047, 2003

Strassmeier, K. G., Boyd, L. J., Epand, D. H.,& Granzer, T. H. 1997, PASP, 109, 697

Viskum, M., Kjeldsen, H., Bedding, T. R., et al. 1998, A&A 335, 549

Zima, W., Heiter, U., Cottrell, P. L., et al. 2003, in Asteroseismology across the HR Diagram, eds. M. J. Thompson, M. S. Cunha, M. J. P. F. G. Monteiro, Kluwer Academic Publishers, 489